Transcriptomic and metabolomic profiling provide insight into the role of sugars and hormones in leaf senescence of Pinellia ternata

Jialei Chen

chenjialeicjl@163.com

China Academy of Chinese Medical Sciences Institute of Chinese Materia Medica
https://orcid.org/0000-0003-2627-8847

Xiwen Li

China Academy of Chinese Medical Sciences Institute of Information on Traditional Chinese Medicine

xue Feng

China Academy of Chinese Medical Sciences Institute of Chinese Materia Medica

Jialu Wang

China Academy of Chinese Medical Sciences Institute of Chinese Materia Medica

Yifei Pei

China Academy of Chinese Medical Sciences Institute of Basic Theory in Chinese Medicine

li Liu

China Academy of Chinese Medical Sciences Institute of Chinese Materia Medica

ziyi Liu

China Academy of Chinese Medical Sciences Institute of Chinese Materia Medica

Research Article

Keywords: Leaf senescence, Pinellia ternata, sugar metabolism, hormone signaling

Posted Date: January 29th, 2024

DOI: https://doi.org/10.21203/rs.3.rs-3869644/v1

Version of Record: A version of this preprint was published at Plant Cell Reports on April 22nd, 2024. See the published version at https://doi.org/10.1007/s00299-024-03222-x.

Abstract

Pinellia ternata, an environmentally sensitive medicinal plant, undergoes leaf senescence twice a year, affecting its development and yield. However, the underlying mechanism of this phenomenon is still largely unexplored. In this study, a typical senescent population model was constructed, and an integrated analysis of transcriptomic and metabolomic profiles of *P. ternata*was conducted using obviously different leaf senescence phenotypes in this model. The result showed that two key modules associated with leaf senescence based on weighted correlation network analysis (WGCNA) were key components for leaf senescence. Further analysis revealed that genes in these two modules were mainly enriched in sugar and hormone signaling pathways, respectively. A network of unigenes and metabolisms related to the obtained two pathways revealed that D-arabitol and 2MeScZR played key roles in leaf senescence. Additionally, a total of 130 hub genes were discovered in this network, and they were categorized into three classes based on connectivity. A total of 34 hub genes and 13 metabolites were further analyzed through a pathway map, the potential crosstalk between sugar and hormone metabolisms might be an underlying reason of leaf senescence in*P. ternata*. These findings address the knowledge gap regarding leaf senescence in *P. ternata*, providing candidate germplasms for molecular breeding and laying theoretical basis for the realization of finely regulated cultivation in future.

Key Message

The interaction network and pathway map uncover the potential crosstalk between sugar and hormone metabolisms as a possible reason for leaf senescence in *P. ternata*.

1. Introduction

Leaf senescence is a crucial process in plants growth cycle, which has always received significant attention because leaves are the main organs responsible for photosynthesis. The occurrence of leaf senescence leads to a suspension of nutrient accumulation, which significantly impacts crop yield and quality (Zhao et al., 2022). During this process, a noticeable manifestation is yellowing in leaf, caused by a series changes such as the destruction of chloroplast (Bhattacharjee, 2005; Domínguez et al., 2021; Mayta et al., 2019). Exploring the mechanisms underlying leaf senescence is beneficial to realize the precise regulation of crops. Numerous studies have demonstrated that leaf senescence is regulated by various pathways, including the accumulation of reactive oxygen species (ROS) (Zhang et al., 2020; Zhang et al., 2022), recognition of light signals (Paluch-Lubawa et al., 2021; Tian et al., 2020; Wang et al., 2022), and biological clock (Zhang et al., 2018). ROS accumulation is involved in cytotoxic processes that induce programmed cell death (PCD) (Dat et al., 2000; Jajic et al., 2015). Several senescence-associated genes (*SAG*s) have been found to affect the scavenging process of antioxidant enzymes. For example, *WRKY75* promotes the transcription of *CATLASE2* (*CAT2*), suppressing the scavenging of H_2O_2 leads to ROS accumulation (Guo et al., 2017). On the other hand, *CLE14* promotes JUB1-mediated ROS

scavenging to maintain ROS homeostasis (Zhang et al., 2022). In dark conditions, carbon starvation can induce leaf senescence, but this can be alleviated by overexpressing of *miR171b* (Wang et al., 2022). *SlJAZ10* and *SlJAZ11* regulate the SlJAV1-SlWRKY51 (JW) complexes to suppress JA biosynthesis and mediate leaf senescence under dark conditions (Tang et al., 2022). *PIF4* proteins activate *NYE1* during prolonged dark-induced conditions, affecting chloroplast activity and the lighting pathways (Song et al., 2014; Woo et al., 2019). On the biological clock, *TIMING OF CAB EXPRESSION1* (*TOC1*) is a circadian clock oscillator in potatoes (Morris et al., 2019), and older leaves have a shorter circadian clock. The Evening Complex (*EC*), a core component of the circadian clock, is involved in JA signaling-induced leaf senescence (Zhang et al., 2018), representing a crosstalk between hormone and circadian signaling. Leaf senescence is a complex process involving multiple pathways.

Pinellia ternata (Thunb.) Breit., a perennial herb of the Araceae family, is commonly used in Traditional Chinese medicine (TCM) due to its various activities, such as anti-vomiting, anti-tumor, and anti-bacterial effects (Peng et al., 2022). This plant undergoes twice senescence each year, mainly due to stress and development, respectively. Previous studies have mainly focused on stress-induced leaf senescence, examining it from physiological, transcriptional and genomic methylation perspectives (Chao et al., 2020; Xue et al., 2010). Transcriptome analysis reveals the involvement of *MYB* and *bHLH* gene families in the heat stress response of *P. ternata* (Wang et al, 2023). Exogenous jasmonic acid (JA) and NO have been shown to enhance the resistance of *P. ternata* to heat stress (Wang et al., 2010; Xue et al., 2008). These studies preliminarily elucidated the reason for stress-induced leaf senescence, and put forward measures to delay leaf senescence. However, despite the extensive research on stress induced leaf senescence in *P. ternata*, there is also a need for studies on age-induced leaf senescence of this plant, which is equally important and deserves further investigation.

This study investigated developmental leaf senescence of *P. ternata* based on the model of plant populations with early and late senescence phenotype at the transcriptional and metabolic levels. The active senescence signaling pathways, hormone and sugar metabolisms were identified in *P. ternata*. Several hub genes and compounds associated with the senescence process were discovered. This research sheds light on the regulatory mechanisms of leaf senescence in *P. ternata*, and provides valuable genetic resources for understanding the process of developmental senescence.

2. Materials and methods

2.1 Plant materials

P. ternata is a herbaceous plant that consists of tuber and root system in the underground part and the above-ground part of petiole, bulbil and leaf (Fig. S1). The senescence in *P. ternata* showed significant dumping and yellowing of the above-ground part. Thirty different populations were used to construct a senescent population model. In this model, four populations of *P. ternata* with significant differences in senescence time (45 days) and stably inherited were used in this study. Among them, ES1 and ES2 were two early leaf senescent populations, LS1 and LS2 were two stay-green populations. Plant materials

were planted on the 28th of March in Anshan County experimental field, tubers were soaked with 0.2% carbendazim (Guoguang) solution before seeding. Obvious differences in leaf senescence phenotype occurred on the 145th day after sprouting. Leaves of each population were collected for MDA content measurement, RNA extraction, ultrastructure observation, metabolites and hormone detection.

2.2 MDA content measurement

Firstly, 0.5 g the collected leaves were grinded with 5 mL 10% trichloroacetic acid (TCA) in a mortar, then the homogenates were centrifuged at 3000 r·min^{-1} for 10 min. The supernatant was prepared for MDA measurement. Take 2.0 mL of the supernatant obtained to a stoppered test tube (three replicates), add 2.0 mL of 0.5% thiobarbituric acid (TBA) solution. When thoroughly mixed, leave it in a boiling water bath for 20 min, then cooled to room temperature and centrifuged at 3000 r/min for 10 min. The OD values of the supernatant were measured at wavelengths of 532 nm, 600 nm, and 450 nm, respectively. For the control tube, supernatant obtained was replaced with 2 mL of ddH_2O. MDA content was calculated by the following formula: MDA (μmol/g·FW) = 6.45×(OD_{532}-OD_{600}) − 0.56×OD_{450}.

2.3 RNA extraction and RT-qPCR analysis

The RNA easy fast plant tissue kit (TIANGEN BIOTECH (BEIJING) CO., LTD., DP452) was used to extract total RNA from the collected leaves. Subsequently, the quality and purity of the extracted RNA were assessed through 1% agarose gel electrophoresis and NanoDropTM 2000 spectrophotometer (Thermo Fisher, USA). The relative expression levels of *PtSAG39* were analyzed using RT-qPCR (Thermo Fisher 7500). *PtGAPDH* was chosen as the internal reference gene, and three biological replicates were conducted with three technical replicates on each sample. The $2^{-\Delta\Delta Ct}$ method was used to calculate the relative expression levels (Livak and Schmittgen, 2001). Primers used in this part can be found in Table S1.

2.4 Ultrastructure of the collected leaves

Leaf samples were carefully cut off from petiole with a scalpel, and then promptly immersed in a 2.5% (V/V) glutaraldehyde solution. Next, the collected leaves were cut into 5 mm×5 mm small pieces and placed into 2 mL centrifuge tubes. After fixing for over 2 hours, the leaf segments were rinsed with PBS three to four times. The samples underwent dehydration using graded ethanol solutions and were subsequently embedded in Epon812 epoxy resin (SPI Company, Batch No. 90529-77-4). The obtained blocks were sectioned into ultra-thin slices by UC7 technology (Leica, Germany). The grids were then stained with uranyl acetate and lead citrate before being examined using a HT7800 transmission electron microscope (Hitachi, Japan).

2.5 Transcriptome data collection and weighted correlation network analysis (WGCNA)

A total amount of 1 μg RNA per sample was used as input material for the RNA sample preparation. Sequencing libraries were generated using NEBNext® UltraTM RNA Library Prep Kit for Illumina® (NEB,

USA) following manufacturer's recommendations. After detection and quantification, high-throughput sequencing was performed on the Illumina HiSeq 2000 platform (NEB, San Diego, CA, USA). The heat-map diagram was sorted by the FPKM value of unigenes and all annotated expression unigenes detected were clustered using TBtools v1.123. Fastp v0.19.3 was used to filter the original data, mainly to remove reads with adapters based on the following strategies, (i) when the N content in any sequencing reads exceeds 10% of the base number of the reads, remove the paired reads; (ii) when the number of low-quality (Q < = 20) bases contained in reads exceeds 50% of the bases of the reads, this paired reads will be removed. Transcriptome assembly was performed using Trinity (v2.11.0). Gene function was further annotated based on the Kyoto Encyclopedia of Genes and Genomes (KEGG). Gene expression levels were calculated the FPKM of each gene based on the gene length.

Co-expression network modules were constructed using TBtools v1.123. To perform cluster analysis on samples and set appropriate thresholds, we employed flash Clust toolkit (R v4.2.1). ES1, ES2, LS1 and LS2 were divided into two groups (ES and LS group) for WGCNA analysis. Three replicates within each group were merged, and then Median Absolute Deviation (MAD) was used for screening. The top 20% of transcripts from the screening results were selected for further WGCNA analysis. Genes with similar expression patterns were classified into the same module, pearson correlation was calculated to determine the relationship between each module and the traits.

2.6 Widely targeted metabolomic analysis

Lyophilized powder of 100 mg leaf tissues was dissolved with 1.2 mL 70% methanol solution, then mixed well. The extraction was analyzed using an UPLC-ESI-MS/MS system (UPLC, SHIMADZU Nexera X2; MS, Applied Biosystems 4500Q TRAP). The analytical condition was as follows, UPLC: column, Agilent SB-C18 (1.8 μm, 2.1 mm×100 mm); The mobile phase was consisted of solvent A (pure water with 0.1% formic acid) and solvent B (acetonitrile with 0.1% formic acid). The flow velocity was set to 0.35 mL per minute; the column oven was 40°C; and the injection volume was 4 μL. The effluent was alternatively connected to an ESI-triple quadrupole-linear ion trap (QTRAP)-MS. The ESI source operation parameters were as follows: source temperature 550°C; ion spray voltage (IS) 5500 V (positive ion mode)/-4500 V (negative ion mode); ion source gas I (GSI), gas II(GSII), curtain gas (CUR) were set to 50, 60, and 25.0 psi, respectively.

2.7 Hormone detection by LC-MS/MS

Internal standard mixture was added in 50 mg leaf tissues of the grinded powder, and 1mL methanol/water/formic acid (15:4:1) was used for hormone extraction. The supernatant was continue to concentrate and redissolve, and then pass through a 0.22 μm filter membrane, the obtained solution was used for LC-MS/MS analysis. The data acquisition instrument system consists of ultra performance liquid chromatography (UPLC) (ExionLC™ AD) and Tandem mass spectrometry (MS/MS) (QTRAP® 6500+). These include a liquid chromatography column: Waters ACQUITY UPLC HSS T3 C18 column (1.8 μm, 100 mm×2.1 mm id); mobile phase: phase A, ultrapure water (with 0.04% acetic acid added); phase B, acetonitrile (with 0.04% acetic acid added); The mass spectrometry conditions mainly include

electrospray ionization source (ESI), temperature 550°C, curtain gas (CUR) 35 psi. In Q-Trap 6500+, each ion pair was scanned and detected according to the optimized declustering potential (DP) and collision energy (CE). The significance of hormone metabolites was determined by the hypergeometric test *P*-value.

2.8 Establishment of gene-metabolite co-expression networks

Hub gene commonly refers to a gene with a high degree of connectivity within co-expression modules. This connectivity is measured by module membership (MM), which is the correlation between gene expression and its corresponding module eigengene (MEs). Gene significance (GS) refers to the correlation of each gene to the traits. To identify candidate genes for further analysis, we focused on the module of interest. Gene-metabolites interaction networks were displayed by Cytoscape (v3.9.1).

2.9 Statistical analysis

Statistical analysis was conducted by GraphPad Prism 8.0 software. The data was presented as mean ± standard error with three biological replicates. SPSS24.0 (SPSS Inc., USA) was used for one-way ANOVA analysis.

3. Result

3.1 Significant differences in leaf senescence phenotype exhibited in ES and LS groups of *P. ternata*

In this study, two germplasms of *P. ternata* with extreme leaf senescence phenotypes (senescent and stay-green) were selected, and the senescent phenotype of each plant was statistically analyzed (Fig. 1a,b). The leaf phenotypes were classified into four types, namely green, green-yellow, yellow and brown. The results showed that yellow and brown were the main leaf types in the leaf senescence group, which accounted for 99% and 97.4% of the total leaf area in ES1 and ES2, respectively. The main leaf type of the stay-green group was green, which accounted for 99.6% and 99.5% of the total leaf area in LS1 and LS2, respectively. In summary, significant differences of leaf senescence phenotypes exhibited between ES and LS groups.

Differences in the ultrastructure of leaves collected were also compared between leaf senescence and stay-green groups. It was found that chloroplast from leaves of ES1 and ES2 were significantly damaged, and the extent was much greater than LS1 and LS2. Moreover, some thylakoids appeared blurred in the chloroplast of ES1 and ES2. The grana thylakoids were observed to be stacked and deformed, and a significant concentration of osmophilic particles was found in the chloroplast. However, chloroplasts of LS1 and LS2 were evenly distributed, the grana and matrix lamellae of chloroplast were complete, and the osmophilic particles had a uniform electron density (Fig. 1c).

Further, the antioxidant properties of *P. ternata* with different leaf senescence phenotypes were compared, and it was found that MDA content in the stay-green group was significantly lower than those in the leaf senescent group, indicating that the membrane lipid peroxidation degree of plants in the stay-green group was less (Fig. 1d). Moreover, leaf senescence marker gene *SAG39*, encoding a cysteine protease, was also analyzed in ES and LS groups (Fig. 1e). Quantitative RT-PCR analysis showed that *PtSAG39* was highly expressed in leaf senescent group (ES1 and ES2), and the relative expression was 427 times higher than that in stay-green group (LS1 and LS2). Additionally, the content of uridine in LS group was significantly higher than that in ES group (Fig. 1f).

3.2 Senescence-related modules obtained by weighted co-expression network analysis

To clarify the reasons for the generation of these two different leaf senescent phenotypes at the transcriptional level. Transcriptome sequencing was conducted in *P. ternata*. After filtration, an average of 53,950,325 clean reads were identified, and 97.12 Gb clean data were obtained. Each sample had a Q30 score of at least 93.75% (Table S2), and 233,993 unigenes were detected (Table S3). The identified transcripts were analyzed by PCA analysis. It showed that samples in ES and LS groups formed separate clusters, and the correlation of gene expression levels was higher within the three biological replicates of each group (Fig. S2).

Further, WGCNA was conducted to identify the co-expressed unigenes between stay-green and non-stay-green traits. To avoid inter-individual variation, we removed 61,363 unigenes specific in ES1 and 64,913 unigenes specific in ES2, and retained 66,419 genes in common for subsequent analysis (Table S4). Similarly, after removing unigenes that were only presented in LS1 (45,972 unigenes) and LS2 (51,337 unigenes), we analyzed the remaining 59,100 common unigenes obtained (Table S5). Subsequently, the de-duplication process was performed on these 66,419 and 59,100 unigenes, and FPKM values of 85,561 unigenes were input into the following noise removal process. Finally, a total of 16,600 unigenes remaining were input to WGCNA shiny for further analysis. The WGCNA analysis parameters were set as follows: the WGCNA ‘module cut tree height’ was set as 0.25; ‘min module gene’ was set as 100; soft power was chosen at 6 (Fig. 2a, Fig. S3a). Here, non-stay green (ES1, ES2) and stay green (LS1, LS2) were taken as trait data to analyze gene module-traits correlations. We achieved an independence score of 0.8 and observed higher average connectivity, the individual samples were well clustered under the soft threshold (Fig. S3). A total of 12 distinct modules marked with different colors were produced according to the similar co-expressed trends of each unigene. The number of unigenes per module were ranged from 107 (green-yellow) to 6,496 (turquoise) (Fig. 2b and Table S6). Module-traits relationships were provided in Fig. 2c, which summarizes the correlation between gene expression and traits in each module. Negative correlation was indicated by purple and positive correlation was indicated by progressive yellow. Among the 12 modules obtained, expression trends of unigenes in the same group (ES or LS) were similar in turquoise and blue modules, and unigenes in these two modules showed opposite expression patterns in ES and LS groups, respectively (Fig. S4). Combined with leaf senescence

phenotype differences in ES and LS, these two modules were considered as senescence-related (SR) modules for further analysis.

3.3 Further analysis of unigenes in SR modules

In the obtained two SR modules, there were 6,496 unigenes in the turquoise module, the expression level of most unigenes in ES group was higher than those in LS group (Fig. 3a). These unigenes were significantly enriched in carbon metabolism, galactose metabolism, carbon fixation in photosynthetic organisms, fructose and mannose metabolism (Fig. 3b). In the blue module, 3984 unigenes exhibited different transcript abundance between ES and LS were shown in Fig. 3c, expression level of most unigenes in ES group was higher than those in LS group. These unigenes were significantly enriched in plant hormone signaling pathways (Fig. 3d).

Notably, photosynthesis related processes were significantly enriched in the two SR modules, which was consistent with the characteristics of leaf senescence phenotype. In addition, we noticed that many metabolic pathways were closely related to sugar metabolism in the turquoise module, and genes in the blue module were significantly enriched in the hormone signaling pathway. It is noteworthy that sugar metabolism and hormone signaling played key roles in leaf senescence (Woo et al., 2018; Woo et al., 2019). An in-depth analysis of these two pathways might provide insights into the underlying mechanism of leaf senescence phenotype.

3.4 Analysis of sugar and hormone content between ES and LS.

In order to further analyze the key metabolic pathways, widely targeted metabolomic analysis and the measurement of hormone contents were performed. Principle component analysis (PCA) of the metabolite profiles showed that ES and LS were separated by PC1 (40.30%) (Fig. S5). A total of 80 sugars and 72 hormones were successfully identified (Fig. 4a, Table S7). Among them, 48 metabolites related to sugar metabolism were further analyzed (Fig. 4a, b). There are 29 metabolites showed higher contents in ES than those in LS group, such as such as D-galacturonic acid (7.03 times), xylitol (2.67 times) and D-arabitol (2.58 times). In addition, according to the result of KEGG enrichment analysis in the blue module, the contents of hormone were analyzed, and a total of 24 hormones showed significant differences between ES and LS groups (Fig. 4c). Among them, the contents of almost all hormones were higher in ES than that in LS group, such as ABA (5.84-fold), MeIAA (4.51-fold) and ACC of ETH (1.60-fold) in ES group. However, some of CKs (K9G, K and mT9G) had higher contents in LS group compared to ES group, including the K9G (0.52-fold), K (0.59-fold) and mT9G (0.49-fold) of salicylic acid. Studying the effects of these metabolites will be beneficial for further understanding the leaf senescence process of *P. ternata*.

3.5 Co-expression network analysis of genes and metabolites involved in sugar and hormone signaling pathways

To sieve the hub genes and metabolites of sugar metabolism and hormone signaling, a co-expression network was constructed using 451 unigenes, 80 metabolites related to sugar metabolism and 24 plant hormones (Fig. 5). By setting the condition that the correlation value between genes and metabolite (0.8) and the *P*-value (0.05), respectively, the unigenes that were not highly correlated with metabolites were removed. 187 genes significantly related to these two pathways were identified. Among them, a number of 130 unigenes were both related to sugar and phytohormone. Additionally, 27 unigenes were only related to sugar metabolism, and 30 unigenes were only related to hormone signaling (Table S8). According to the connectivity between unigenes and metabolites, the obtained 130 common unigenes were further divided into three categories, including level (connectivity ≥ 10), level (10 > connectivity ≥ 5), and level (connectivity < 5) (Table S9). According to the connectivity of 33 core metabolites in the correlation network, the top 8 sugars and hormones with the highest connectivity were selected respectively for further analysis (Table S10). Of the 130 genes, 117 unigenes were significantly associated with these hub metabolites (Table S8).

3.6 Potential mechanism underlying leaf senescence phenotype between ES and LS groups.

The 16 hub metabolites were mapped onto the sugar metabolism and plant hormone signaling pathway by combining the metabolic components and related unigenes in the KEGG pathway shown in Fig. 6. We overlapped 117 genes with the unigenes annotated in the regulatory network to obtain 34 genes. According to the connectivity classification of 34 genes, the genes of , andlevel were marked with 3, 2 and 1 asterisks respectively.

In sugar metabolism pathway, the contents of sucrose, melibiose, maltose and trehalose were lower in ES group than those in LS group. The contents of arabitol, xylitol, maltotetraose and glycerophosphoinositol were higher in ES group than those in LS group. The expression level of genes encoding key sugar biosynthetic enzymes, including sucrose synthase (SUS), stachyose synthetase (STS1), and galactinol synthase 1-like (GOLS) in LS group were higher than that in ES group. However, the expression levels of four UGE genes (Cluster-21316.3, Cluster-21316.5, Cluster-70037, and Cluster-84086.4) and two RFS genes (Cluster-83480.3, and Cluster-90151.3) were higher in ES group, while those of one other RFS genes (Cluster-49308.32) were lower in LS group. The direct product of RFS action, raffinose, was not detected in the assayed samples (Fig. 6).

In plant hormone signaling pathway, the contents of the seven hormones were higher in ES group than those in LS group. These metabolites included ABA, ETH (ACC), auxin (IA and IAA-Val-Me), and CKs (2MeScZR, IPR and K9G). The level of SLs (5-DS) was lower in ES group than that in LS group. Hormone is an important signal substance for regulating leaf senescence. Genes encoding abscisic acid receptor PYL (Cluster-77899.0 and Cluster-77899.2), auxin-responsive protein IAA (Cluster-28979.2, Cluster-50616.2), auxin response factor ARF (Cluster-55946.1, Cluster-58994.0), and transcription factor GLK1 (Cluster-73416.0) were key components in this pathway. The expression of these genes were higher in LS group, which were negatively correlated with the levels of ABA, auxin and CKs. Additionally, the

expression levels of genes encoding serine/threonine-protein kinase CTR1 (Cluster-76788.0), three auxin responsive GH (Cluster-85099.4, Cluster-85099.5, and Cluster-85099.8), five auxin-response protein SAUR (Cluster-12894.3, Cluster-21438.4) in ES group were higher compared to those in LS group, which were positively correlated with the levels of ETH and auxin.

4. Discussion

Leaf senescence is a form of PCD that involves the degradation of chlorophyll. It is a crucial developmental process that transfers nutrients from leaves to other organs, promoting plant growth and crop productivity. *P. ternata* is a herbaceous plant whose leaves are the main organs that produce photosynthetic products. The leaf senescence of *P. ternata* is a complex regulatory process that involves the coordinated action of multiple pathways. Therefore, it is essential to comprehend how senescence signals are perceived and processed in *P. ternata* leaves and to understand the mechanisms of senescence regulation. This work will aid in the development of refined cultivation and management strategies. In this study, two natural leaf senescence model populations of *P. ternata* were constructed, including early leaf senescent populations (ES) and stay-green populations (LS). The integrated analysis of transcriptome and metabolome analysis revealed that sugar and hormone metabolisms were the underlying reason for leaf senescent differences between ES and LS groups. Comparatively to LS group, germplasms in ES group displayed more overt signs of leaf senescence, which was reflected by the changes in physiological activities, chloroplast damages, the content of sugar and hormone and the expression levels of *SAG*s.

Sugars are a vital messenger in the regulation of plant development. There were few studies on sugar metabolism in leaf senescence of *P. ternata*. To understand the roles of sugar in ES and LS groups, we analyzed gene expression levels and contents of sugar related metabolites in these groups. It showed that the expression levels of *Galactinol synthase 1* (*GOLS1*), *Galactinol synthase 2* (*GOLS2*) and *raffinose synthase* (*RFS*) in LS showed higher expression levels compared to those in ES group. This trend was similar to the changes in leaf senescence in grapes (Ma et al., 2023). Interestingly, Raffinose family oligosaccharides (RFOs) are worthwhile for plant growth and development that function as osmoprotectants. GOLS and RFS are critical enzymes involved in RFO biosynthesis (Jing et al., 2023). The expression levels of UDP-glucose 4-epimerase-related genes *UGE1, UGE5* and *RFS6* in leaves of ES group, displayed higher expression levels compared to those in LS group. In this study, the relative content of galactinol in ES group was significantly lower than that in LS group. Galactinol and raffinose effectively protected salicylate from hydroxyl radical attack in vitro. These findings suggest the possibility that galactinol and raffinose scavenge hydroxyl radicals as a novel function to protect plant cells from oxidative damage during leaf senescence in *P. ternata* (Nishizawa et al., 2008).

Previous research indicated that D-Arabitol is involved in the metabolism of pentose phosphate degradation and suggested that the photosynthesis of senescent leaves was inhibited. Glycerophosphoinositol (PIs) is an extra-plastidial lipid that plays a crucial role as a signaling lipid, transporting materials and maintaining cell plant structure. The increased accumulation of PI lipid

classes in ES during leaf senescence may indicate the plant's efforts to cope with the stress caused by this process (Ciubotaru et al., 2023). Carbohydrates, including Xylitol (Maaloul et al., 2021)d Maltotetraose (Liang et al., 2021), primarily regulate osmotic pressure in plant cells and protect biological membranes. The present findings suggest that carbohydrates could play a significant role in investigating the leaf senescence of *P. ternata*.

Phytohormones play a role in leaf senescence in plants. However, the intricate regulatory mechanisms involved in leaf senescence in *P. ternata* remain unclear. To comprehend the hormone roles between ES and LS groups, we analyzed hormone content and the expression levels of related genes.

Abscisic acid (ABA) plays an essential role in leaf senescence. In the current investigation, ES exhibited a significantly higher level of ABA content than LS. The expression levels of two ABA signaling and response-related genes *PYL3* and *PYL9* were lower in ES leaves compared to LS. Ethylene and strigolactone (SL) promote senescence and abscission of plant leaves. In this study, ETH and SL contents in ES group showed significantly higher levels compared to LS group. SLs could modulate the capacity of leaves to capture light energy by altering the components of photosynthetic pigments (Alvi et al., 2022). Further studies on the role of ETH and SLs in controlling chloroplast degradation during leaf senescence are needed. Auxin regulates cell enlargement and plant growth, but the role of auxin in leaf senescence is complex, and the potential mechanism is still much less understood. In this study, ES showed significantly higher expression levels of IA and IAA-Val-Me contents compared to the LS. This phenomenon was similar to that observed in senescent leaves of *Arabidopsis thaliana*, where free IAA levels were significantly higher than that in non-senescent leaves (Quirino et al., 1999). The expression levels of auxin signaling and response-related genes *IAAs*, *ARFs* in leaves of ES, showed lower expression levels compared to LS group. In previous studies, IAAs and ARFs were considered as negative regulators of auxin signaling, with expression levels decreasing with aging (Ellis et al., 2005; van der Graaff et al., 2006). Meanwhile, the results of the expression of auxin signaling and response-related genes *GH3s*, *SAURs* in leaves of ES showed higher expression levels compared to the LS. This trend is also consistent with studies in *Arabidopsis thaliana*, where *AtGH3.1*, a member of the GH3 family involved in the early response to auxin, was up-regulated in senescent leaves (Buchanan-Wollaston et al., 2005). Similarly, *AtSAUR36*, a member of the SAUR family involved in the early response to auxin, positively regulates leaf senescence (Bemer et al., 2017; Hou et al., 2013). The traditional concept is that auxin is a negative regulator of leaf senescence. In recent years, more experimental evidence has shown that auxin is a positive regulator of leaf senescence (Mei et al., 2019). Interestingly, the auxin levels and expression levels of related genes in senescent leaves of *P. ternata* in this study also support the argument that auxin may be a positive regulator during leaf senescence. CK has an anti-senescence effect by increasing the antioxidant activity, the content of chlorophyll, and protein in the plant. The cytokinin signaling and response related genes HK5, CKI1, GLK1, RR1 were lower in ES leaves compared to LS. This effect proves that the degree of senescence of ES leaves was more severe (Peng et al., 2021).

Many plants rely on intricate crosstalk between nutrients and hormones, an effective way of coupling nutritional and developmental information and adjusting their growth and senescence (Singh and

Roychoudhury, 2023). Sugar and hormones are thought to work synergistically to regulate plant growth, development and environmental responses (Hu et al., 2017). Sugars in their different forms such as sucrose, glucose, fructose and trehalose-6-P and the hormone family are major regulators of the shoot and root functioning throughout the plant life cycle (Qian et al., 2020). Their combined effects have unexpectedly received little attention, resulting in many gaps in current knowledge. In Fig. 5, we tried to establish the crosstalk of sugar metabolism and hormone signaling pathways, and summarize gene and metabolite changes. The current theory in plant research could explain the synergistic relationship between sugar and ABA signaling, that high sugar levels in plants can increase ABA synthesis and activate the ABA signaling pathway (Arenas-Huertero et al., 2000). The T6P-SnRK1 pathway and sugar-ABA interaction are thought to be involved in processes such as plant senescence (Liu et al., 2023). ABA signaling is involved in regulating leaf senescence by T6P and SnRK1 pathways. Several studies have reported that the sugar signal of T6P directly inhibited SnRK1 activity in vitro both in *Arabidopsis* and wheat grains. In our study, the Tre and T6P contents of LS leaves were relatively higher than those of ES, and the expression levels of genes related to its ABA signaling pathway were also significantly higher than those of ES. This trend is consistent with wheat grains during senescence and irrigation. Further study demonstrated that Tre metabolic pathway might be the central regulatory system for sucrose allocation and sugar–ABA interactions in wheat grains. These findings suggest that accelerating the biosynthesis or signal transduction of senescence-related hormones at grain filling may be one of the ways via which TaTPP-7A synchronously enhanced grain filling and maturation. Based on the above experimental results, it is suggested that future work should investigate whether the signaling regulation of leaf senescence in *P. ternata* is also related to the process of nutrient sucrose storage during the maturation stage.

In this study, we constructed a population model with different natural senescent processes and comprehensively analyzed them from physiology, cytology, transcriptome and metabolomics. Based on this model, we investigated the hub genes and metabolites that are closely related to the natural leaf senescence process. In the next step, we will focus on the functional validation of key genes related to sugar and hormone signaling. Additionally, we will also investigate whether exogenous application of key metabolites could maintain metabolic homeostasis in *P. ternata* to delay leaf senescence at a certain time.

5. Conclusion

In summary, this study reveals that the natural leaf senescence process of *P. ternata* is closely related to the regulation of sugar and hormone metabolism. Key sugars, hormones and their associated genes that induce leaf senescence in *P. ternata* were identified. These results can provide insight into the regulation mechanism of the natural leaf senescence process, offering important information for the cultivation and management of *P. ternata*.

Declarations

Funding

This work was supported by grants from the Scientific and Technological Innovation project of China Academy of Chinese Medical Sciences (CACMS Innovation Fund CI2021A04106, CI2021A03910), the Fundamental Research Funds for the Central public welfare research institutes of China (ZXKT21026, ZZ15-YQ-033, ZXKT23004), and the Major Special Project of Scientific and Technological Cooperation of Bijie City (2021-02).

CRediT authorship contribution statement

Jialei Chen: Writing - Original Draft, Investigation, Data Curation, Formal Analysis, Resources,Visualization; Jialu Wang: Writing - Original Draft, Formal Analysis, Validation, Visualization; Li Liu: Investigation, Methodology, Resources; Yifei Pei: Visualization; Ziyi Liu: Resources; Xue Feng: Conceptualization, Funding Acquisition, Validation, Supervision, Methodology, Writing-Review & Editing; Xiwen Li: Funding Acquisition, Supervision, Writing-Review & Editing.

Declaration of Competing Interests

The authors declare no conflict of interest.

Data availability

The raw data that supports the findings of this study are available in National Center for Biotechnology Information (NCBI, https://www.ncbi.nlm.nih.gov). The associated BioProject, BioSample, and SRA numbers are PRJNA1056149, SAMN39090724, and SRR27334041, respectively. These data were released on October 1, 2024.

References

1. Alvi AF, Sehar Z, Fatma M, Masood A, Khan NA (2022) Strigolactone: an emerging growth regulator for developing resilience in plants. Plants (Basel Switzerland) 11. https://doi.org/10.3390/plants11192604
2. Arenas-Huertero F, Arroyo A, Zhou L, Sheen J, León P (2000) Analysis of Arabidopsis glucose insensitive mutants, *gin5* and *gin6*, reveals a central role of the plant hormone ABA in the regulation of plant vegetative development by sugar. Genes Dev 14(16):2085–2096
3. Bemer M, van Mourik H, Muiño JM, Ferrándiz C, Kaufmann K, Angenent GC (2017) FRUITFULL controls *SAUR10* expression and regulates arabidopsis growth and architecture. J Exp Bot 68:3391–3403. https://doi.org/10.1093/jxb/erx184
4. Bhattacharjee S (2005) Reactive oxygen species and oxidative burst: roles in stress, senescence and signal transduction in plants. Curr Sci 89:1113–1121
5. Buchanan-Wollaston V, Page T, Harrison E, Breeze E, Lim PO, Nam HG, Lin JF, Wu SH, Swidzinski J, Ishizaki K, Leaver CJ (2005) Comparative transcriptome analysis reveals significant differences in

gene expression and signalling pathways between developmental and dark/starvation-induced senescence in Arabidopsis. The Plant J 42:567–585. https://doi.org/10.1111/j.1365-313X.2005.02399.x

6. Ciubotaru RM, Garcia-Aloy M, Masuero D, Franceschi P, Zulini L, Stefanini M, Oberhuber M, Robatscher P, Chitarrini G, Vrhovsek U (2023) Semi-targeted profiling of the lipidome changes induced by *Erysiphe Necator* in Disease-resistant and *Vitis vinifera* L. Varieties. Int J Mol Sci 24:4072. https://doi.org/10.3390/ijms24044072
7. Chao Q, Liu X, Han L, Ma C, Gao R, Chen Y, Shi J, Xiong Y, Xue T, Xue J (2020) Variation analysis of genomic methylation induced by high temperature stress in *Pinellia ternata*. China J Chin Mater Med 45:341–346. https://doi.org/10.19540/j.cnki.cjcmm.20191104.102
8. Dat J, Vandenabeele S, Vranová E, Van Montagu M, Inzé D, Van Breusegem F (2000) Dual action of the active oxygen species during plant stress responses. Cell Mol Life Sci 57:779–795. https://doi.org/10.1007/s000180050041
9. Domínguez F, Cejudo FJ, Sandalio LM (2021) Chloroplast dismantling in leaf senescence. J Exp Bot 72:5905–5918. https://doi.org/10.1093/jxb/erab200
10. Ellis CM, Nagpal P, Young JC, Hagen G, Guilfoyle TJ, Reed JW (2005) *AUXIN RESPONSE FACTOR1* and *AUXIN RESPONSE FACTOR2* regulate senescence and floral organ abscission in *Arabidopsis thaliana*. Development 132:4563–4574. https://doi.org/10.1242/dev.02012
11. Guo P, Li Z, Huang P, Li B, Fang S, Chu J, Guo H (2017) A tripartite amplification loop involving the transcription factor WRKY75, Salicylic Acid, and Reactive Oxygen Species accelerates leaf senescence. Plant Cell 29:2854–2870. https://doi.org/10.1105/tpc.17.00438
12. Hou K, Wu W, Gan SS (2013) *SAUR36*, a SMALL AUXIN UP RNA Gene, is involved in the promotion of leaf senescence in Arabidopsis. Plant Physiol 161:1002–1009. https://doi.org/10.1104/pp.112.212787
13. Hu Y, Jiang Y, Han X, Wang H, Pan J, Yu D (2017) Jasmonate regulates leaf senescence and tolerance to cold stress: crosstalk with other phytohormones. J Exp Bot 68:1361–1369. https://doi.org/10.1093/jxb/erx004
14. Jajic I, Sarna T, Strzalka K (2015) Senescence, stress, and Reactive Oxygen Species. Plants 4:393–411. https://doi.org/10.3390/plants4030393
15. Jing Q, Chen A, Lv Z, Dong Z, Wang L, Meng X, Feng Y, Wan Y, Su C, Cui Y, Xu W, Hou H, Zhu X (2023) Systematic analysis of galactinol synthase and raffinose synthase gene families in potato and their expression patterns in development and abiotic stress responses. Genes 14. https://doi.org/10.3390/genes14071344
16. Liang Y, Wei G, Ning K, Li M, Zhang G, Luo L, Zhao G, Wei J, Liu Y, Dong L, Chen S (2021) Increase in carbohydrate content and variation in microbiome are related to the drought tolerance of *Codonopsis Pilosula*. Plant Physiol Biochem 165:19–35. https://doi.org/10.1016/j.plaphy.2021.05.004

17. Liu H, Si X, Wang Z, Cao L, Gao L, Zhou X, Wang W, Wang K, Jiao C, Zhuang L, Liu Y, Hou J, Li T, Hao C, Guo W, Liu J, Zhang X (2023) *TaTPP-7A* positively feedback regulates grain filling and wheat grain yield through T6P-SnRK1 signalling pathway and sugar-aba interaction. Plant Biotechnol J 21:1159–1175. https://doi.org/10.1111/pbi.14025
18. Livak KJ, Schmittgen TD (2001) Analysis of relative gene expression data using real-time quantitative PCR and the 2(-Delta Delta C(T)) method. Methods (San Diego. Calif) 25:402–408. https://doi.org/10.1006/meth.2001.1262
19. Ma W, Lu S, Li W, Nai G, Ma Z, Li Y, Chen B, Mao J (2023) Transcriptome and metabolites analysis of water-stressed grape berries at different growth stages. Physiol Plant 175:e13910. https://doi.org/10.1111/ppl.13910
20. Maaloul S, Abdellaoui R, Mahmoudi M, Bouhamda T, Bakhshandeh E, Boughalleb F (2021) Seasonal environmental changes affect differently the physiological and biochemical responses of two *Limonium* species in *Sabkha Biotope*. Physiol Plant 172:2112–2128. https://doi.org/10.1111/ppl.13446
21. Mayta ML, Hajirezaei M, Carrillo N, Lodeyro AF (2019) Leaf senescence: the chloroplast connection comes of age. Plants 8:495. https://doi.org/10.3390/plants8110495
22. Morris WL, Ducreux LJM, Morris J, Campbell R, Usman M, Hedley PE, Prat S, Taylor MA (2019) Identification of *TIMING OF CAB EXPRESSION 1* as a temperature-sensitive negative regulator of tuberization in potato. J Exp Bot 70:5703–5714. https://doi.org/10.1093/jxb/erz336
23. Mei Y, Wen Z, Wang N (2019) Auxin and leaf senescence regulation. Sci China Ser C 49:1119–1124. https://doi.org/10.1360/SSV-2019-0157
24. Nishizawa A, Yabuta Y, Shigeoka S (2008) Galactinol and raffinose constitute a novel function to protect plants from oxidative damage. Plant Physiol 147:1251–1263. https://doi.org/10.1104/pp.108.122465
25. Paluch-Lubawa E, Stolarska E, Sobieszczuk-Nowicka E (2021) Dark-induced barley leaf senescence – a crop system for studying senescence and autophagy mechanisms. Front Plant Sci 12. https://doi.org/10.3389/fpls.2021.635619
26. Peng K, Zhang W, Zhu X, Zhang K (2021) Research progress on the mechanisms of cytokinin-inhibited leaf senescence. Plant Physiol Commun 57:12–18. https://doi.org/10.13592/j.cnki.ppj.2020.0149
27. Peng W, Li N, Jiang E, Zhang C, Huang Y, Tan L, Chen R, Wu C, Huang Q (2022) A review of traditional and current processing methods used to decrease the toxicity of the rhizome of *Pinellia ternata* in traditional Chinese medicine. J Ethnopharmacol 299:115696. https://doi.org/10.1016/j.jep.2022.115696
28. Qian Y, Cao L, Zhang Q, Amee M, Chen K, Chen L (2020) SMRT and Illumina RNA sequencing reveal novel insights into the heat stress response and crosstalk with leaf senescence in tall fescue. BMC Plant Biol 20. https://doi.org/10.1186/s12870-020-02572-4

29. Quirino BF, Normanly J, Amasino RM (1999) Diverse range of gene activity during Arabidopsis thaliana leaf senescence includes pathogen-independent induction of defense-related genes. Plant Mol Biol 40:267–278. https://doi.org/10.1023/a:1006199932265
30. Singh A, Roychoudhury A (2023) Abscisic acid in plants under abiotic stress: crosstalk with major phytohormones. Plant Cell Rep 42:961–974. https://doi.org/10.1007/s00299-023-03013-w
31. Song Y, Yang C, Gao S, Zhang W, Li L, Kuai B (2014) Age-triggered and dark-induced leaf senescence require the bHLH transcription factors PIF3, 4, and 5. Mol Plant 7:1776–1787. https://doi.org/10.1093/mp/ssu109
32. Tang B, Tan T, Chen Y, Hu Z, Xie Q, Yu X, Chen G (2022) *SlJAZ10* and *SlJAZ11* mediate dark-induced leaf senescence and regeneration. PLoS Genet. 18, e1010285. https://doi.org/10.1371/journal.pgen.1010285
33. Tian T, Ma L, Liu Y, Xu D, Chen Q, Li G (2020) Arabidopsis FAR-RED ELONGATED HYPOCOTYL3 integrates age and light signals to negatively regulate leaf senescence. Plant Cell 32:1574–1588. https://doi.org/10.1105/tpc.20.00021
34. Van der Graaff E, Schwacke R, Schneider A, Desimone M, Flugge U, Kunze R (2006) Transcription analysis of Arabidopsis membrane transporters and hormone pathways during developmental and induced leaf senescence. Plant Physiol 141:776–792. https://doi.org/10.1104/pp.106.079293
35. Wang C, Wang K, Tang X, Tan X, Li C (2010) Effect of exogenous nitric oxideon antioxidant system of *Pinellia ternata* under high temperature stress. Jiangxi Agricultural J 22:41–43
36. Wang JL, Chen JL, Zhang XY, Feng X, Li XW (2023) Physiological and transcriptional responses to heat stress in a typical phenotype of *Pinellia ternata*. Chin J Nat Med 4:243–252. https://doi.org/doi: 10.1016/S1875-5364(23)60433-9
37. Wang K, Cai S, Xing Q, Qi Z, Fotopoulos V, Yu J, Zhou J (2022) Melatonin delays dark-induced leaf senescence by inducing *miR171b* expression in tomato. J Pineal Res 72. https://doi.org/10.1111/jpi.12792
38. Woo HR, Kim HJ, Lim PO, Nam HG (2019) Leaf senescence: systems and dynamics aspects. Annu Rev Plant Biol 70:347–376. https://doi.org/10.1146/annurev-arplant-050718-095859
39. Woo HR, Masclaux DC, Lim PO (2018) Plant senescence: how plants know when and how to die. J Exp Bot 69:715–718. https://doi.org/10.1093/jxb/ery011
40. Xue J, Wang X, Zhang A, Chang L (2008) Effects of salicylic acid on photosynthesis and chlorophyll fluorescence in *Pinellia ternata* leaves under high temperature. Chin Pharm J 43:1855–1858. https://doi.org/10.3321/j.issn:1001-2494.2008.24.005
41. Xue J, Wang X, Zhang A, Chang L (2010) Changes of photosynthesis parameters and chlorophyll fluorescence around sprout tumble of *Pinellia ternata* under high temperature stress China J. Chin Mater Med 35:2233–2235. https://doi.org/10.4268/cjcmm20101703
42. Zhang Y, Wang Y, Wei H, Li N, Tian W, Chong K, Wang L (2018) Circadian evening complex represses jasmonate-induced leaf senescence in Arabidopsis. Mol Plant 11:326–337. https://doi.org/10.1016/j.molp.2017.12.017

43. Zhang Z, Liu C, Guo Y (2020) Wheat transcription factor TaSNAC11-4B positively regulates leaf senescence through promoting ROS production in transgenic Arabidopsis. Int J Mol Sci 21:7672. https://doi.org/10.3390/ijms21207672
44. Zhang Z, Liu C, Li K, Li X, Xu M, Guo Y (2022) CLE14 functions as a brake signal to suppress age-dependent and stress-induced leaf senescence by promoting JUB1-mediated ROS scavenging in Arabidopsis. Mol Plant 15:179–188. https://doi.org/10.1016/j.molp.2021.09.006
45. Zhao W, Zhao H, Wang H, He Y (2022) Research progress on the relationship between leaf senescence and quality, yield and stress resistance in horticultural plants. Front Plant Sci 13. https://doi.org/10.3389/fpls.2022.1044500

Figures

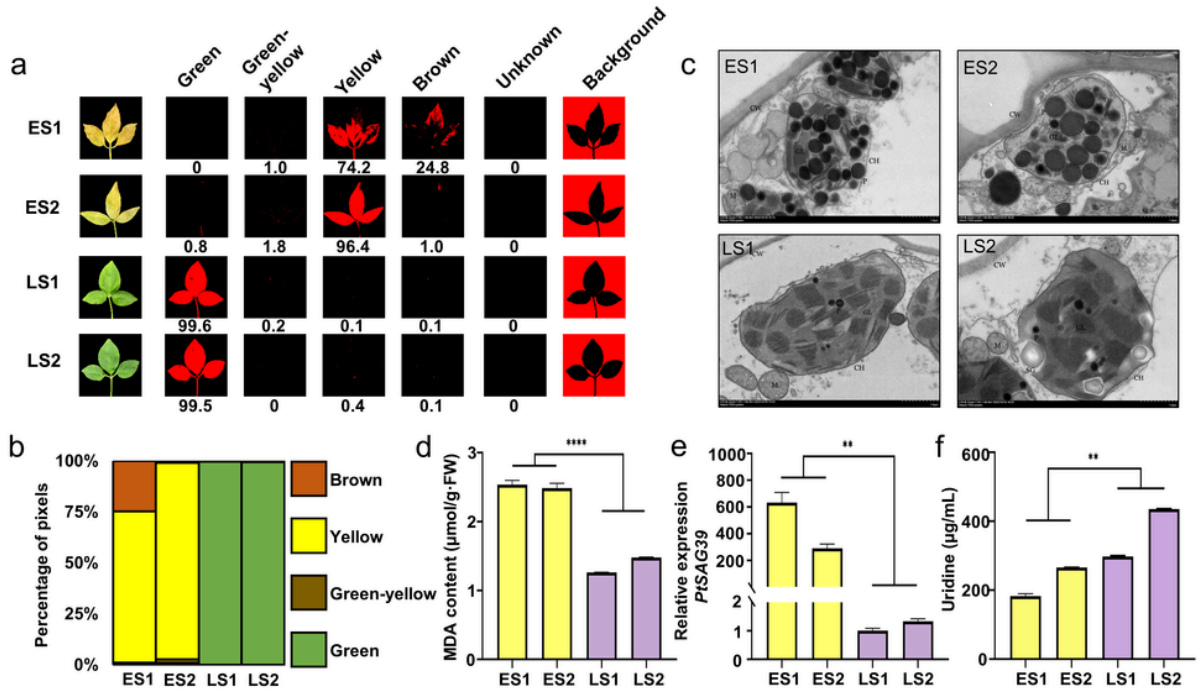

Figure 1

Phenotypic, cytological and physiological differences of leaves between ES and LS groups.
(a-b) Leaf senescence phenotype of the *P.ternata* between ES and LS groups. ES: leaf senescent group; LS: stay-green group. (c) Differences of chloroplast ultrastructure of ES and LS groups. CH: chloroplasts, CW; cell wall, V: vacuole, M: mitochondrion, OG: osmiophilic particles, GL: granum lamella, SL: stroma lamella, S: starch granule. (d) Differences in MDA activities of ES and LS groups. (e) Relative expression levels of marker gene *SAG39* in *P. ternata*, determined by RT-qPCR. (f) The content of uridine in ES and LS

groups. In (d) (e) and (f), asterisks indicate significant differences between ES (ES1, ES2) and LS (LS1, LS2) groups (two-tailed Student's *t* test, ** $P < 0.01$, **** $P < 0.0001$).

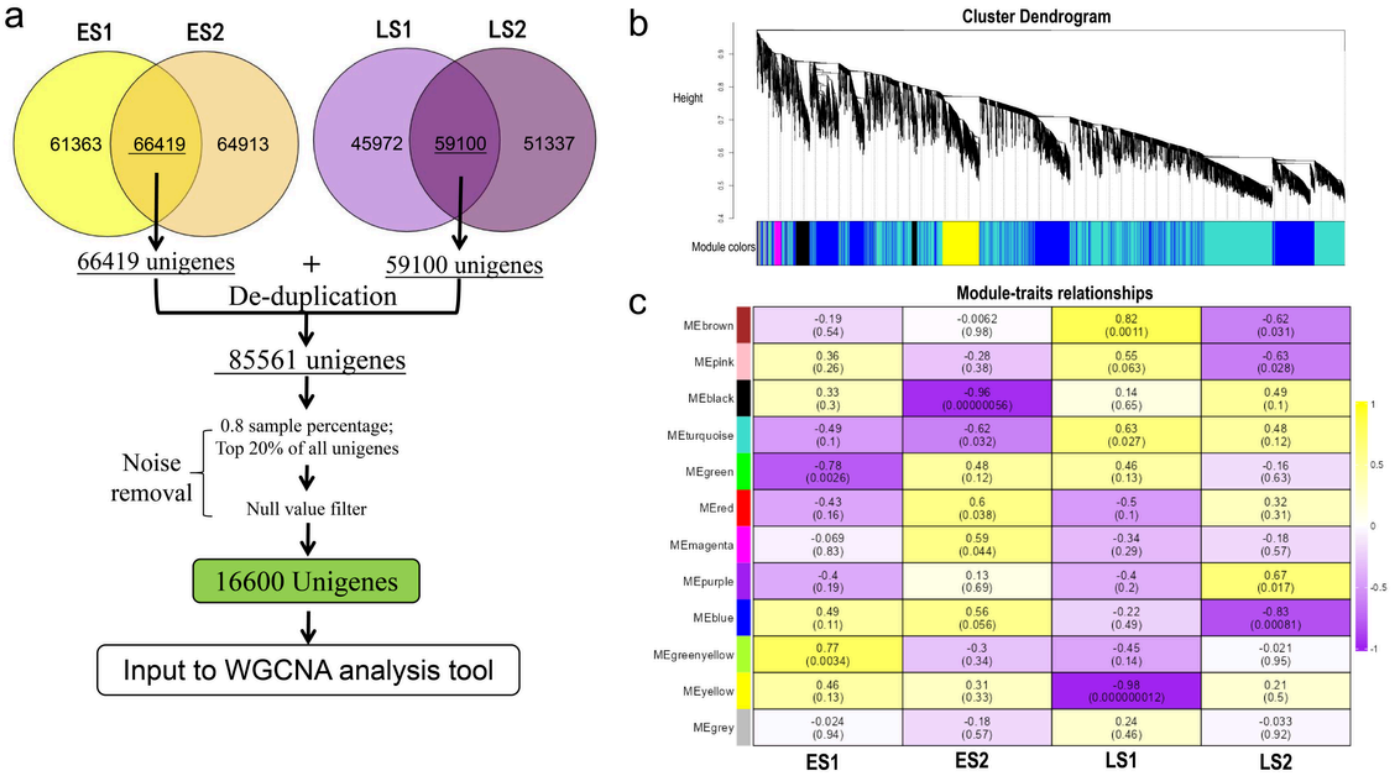

Figure 2

Senescence-related modules in *P. ternata* were obtained by WGCNA.

(a) Data filtering process for WGCNA. Firstly, 59,100 co-expression unigenes in ES1 and ES2, and 66,419 co-expression unigenes in LS1 and LS2 were obtained. Further, duplicate unigenes in these two sets were deleted, the remaining 85,561 unigenes made up the initial set for WGCNA. After noise removal, 16,600 unigenes were finally input to WGCNA shiny.

(b) Clustering dendrogram of the input unigenes, with dissimilarity based on the topological overlap, together with assigned module colors.

(c) Module–trait relationships. The leftmost color block represents different modules, and the rightmost color bar indicates correlation between each module and trait. In the heatmap, yellow represents positive correlation and purple represents negative correlation. Within each cell, the number above indicates correlation, and the number below indicates significance.

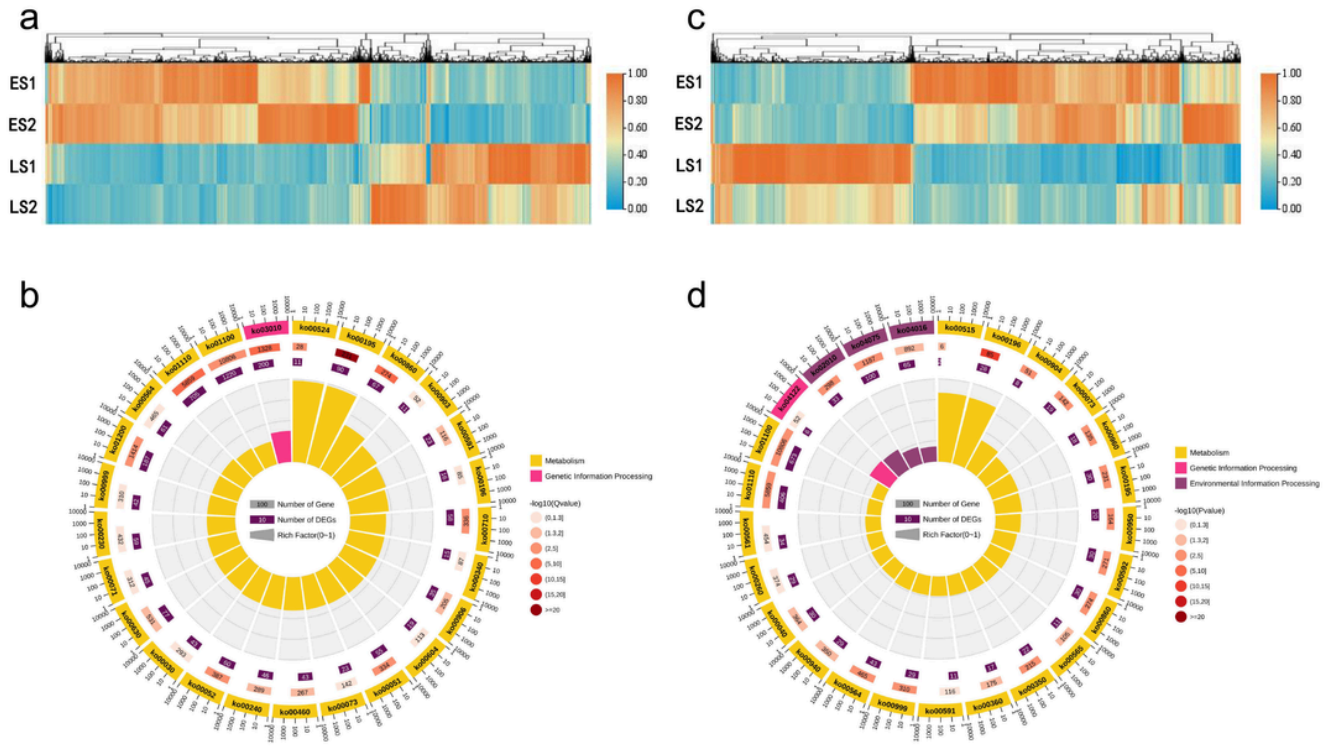

Figure 3

Expression pattern and KEGG enrichment analysis of unigenes in the SR modules.

(a) and (c) Heatmap analysis of all identified genes in turquoise and blue modules; Orange represents higher expression level, and blue indicates lower expression level.

(b) and (d) KEGG analysis and of all identified unigenes in turquoise and blue modules. Circles are viewed from the outside looking in. Circle 1 is the pathway enrichment classification, with the number of genes on the outside of the circle on the scale. Circle 2 indicates that the more genes in this category in the background, the longer the bar chart. Circle 3 shows the total number of genes in the foreground. The higher the significance, the darker the red color. Circle 4 shows the RichFactor value for each pathway-enriched category.

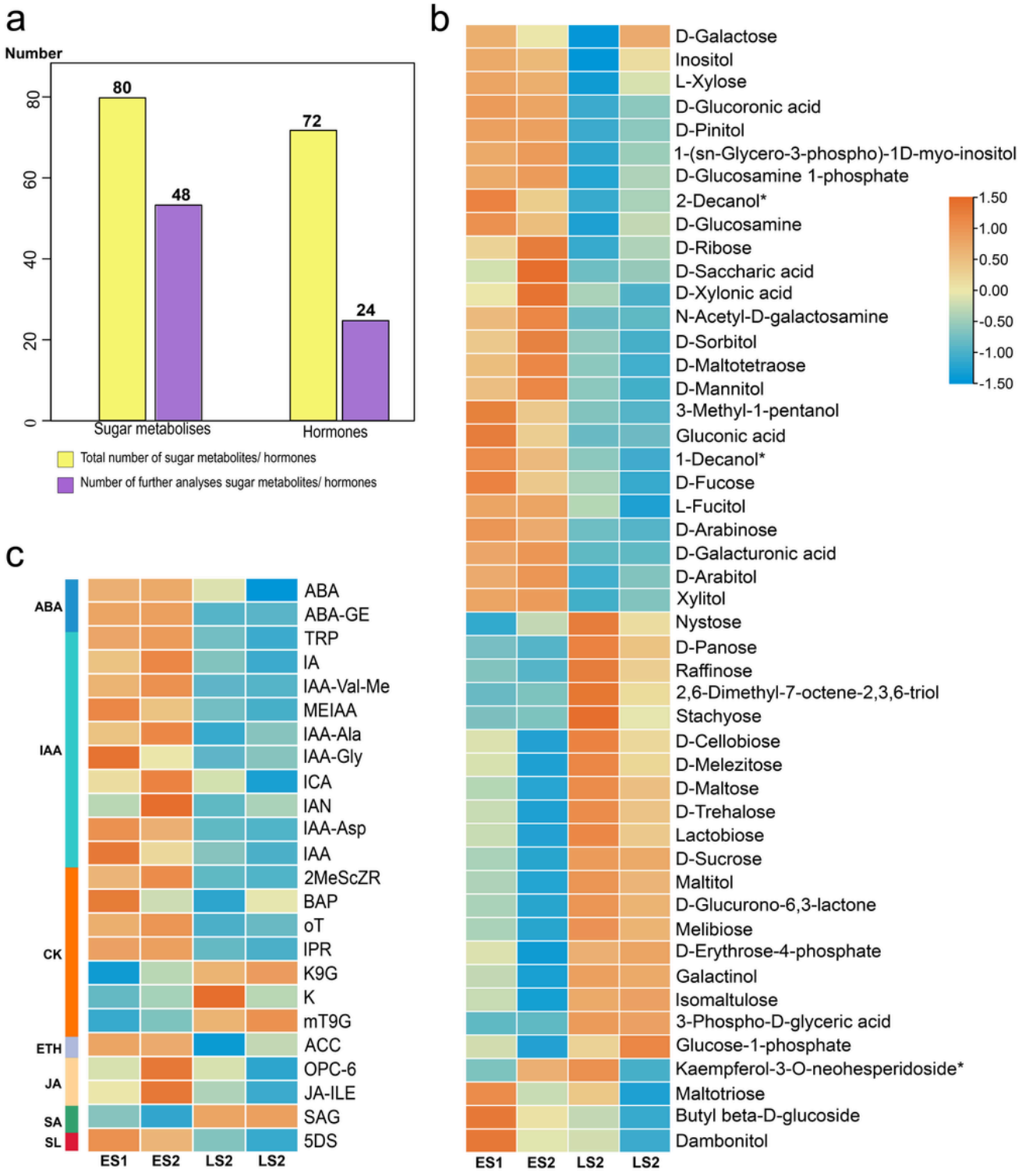

Figure 4

Heat map of overall metabolite percentage, sugar and hormone content.

(a) The number of sugar metabolises and hormones. Two yellow columns indicate the total sugar metabolises and hormones number, respectively. Two grape columns indicate the number of further analyses sugar metabolises and hormones, respectively.

(b) Heat map of metabolites involved in sugar metabolism in ES and LS groups. c: Heat map of hormones in ES and LS groups.

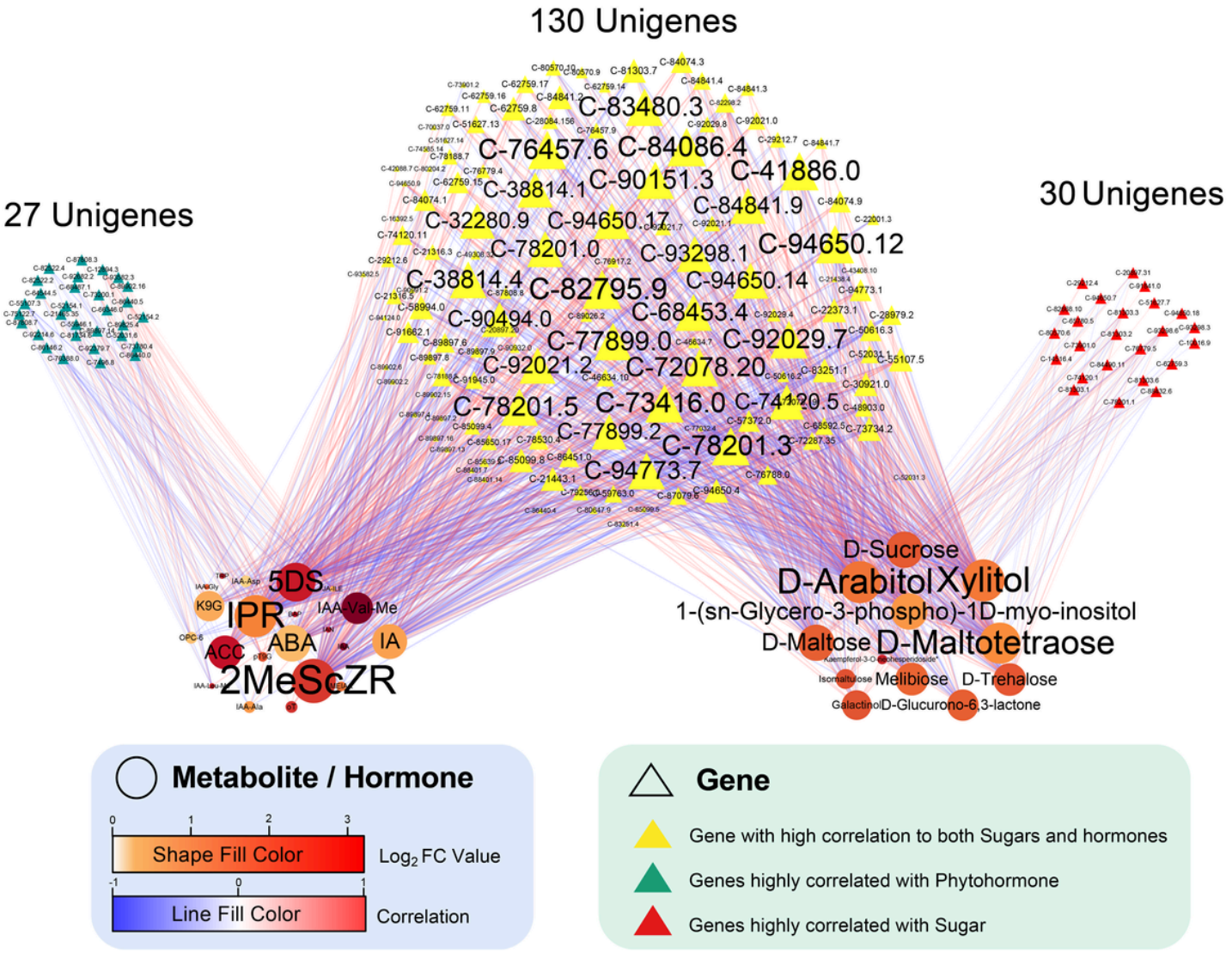

Figure 5

The network of sugars, hormones and their associated unigenes.

Correlation network were constructed on unigenes specifically associated with metabolites. Metabolites are represented by orange circles. Unigenes involved in sugar metabolism pathway are shown as red triangle. Unigenes involved in hormone signaling pathway are shown as green triangle. Other unigenes are shown as yellow triangle, which correlate to both of the above pathways.

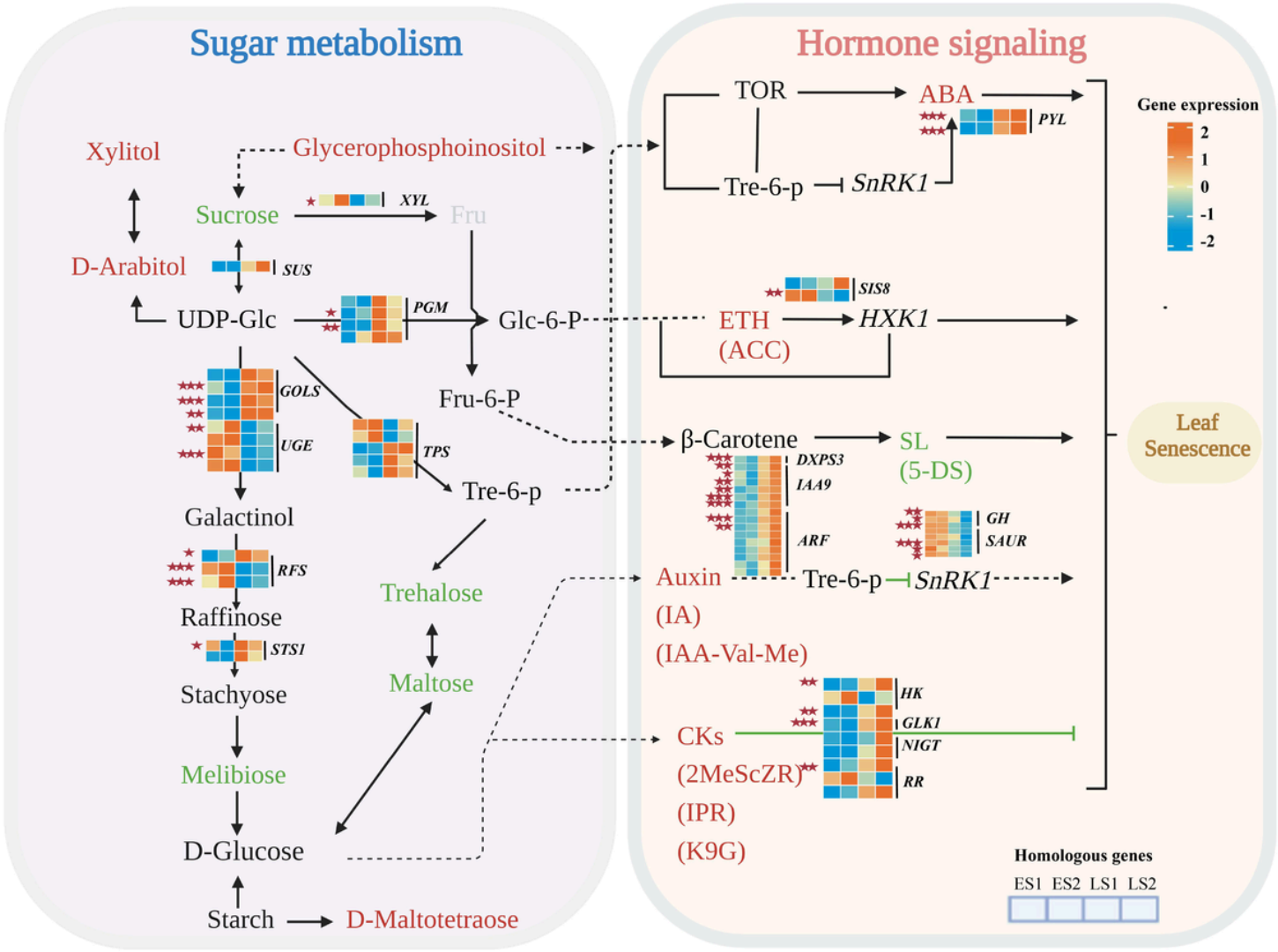

Figure 6

Critical sugar and hormone metabolism mediates leaf senescence.

Metabolites related to sugar and hormone metabolisms were displayed in this figure. Expression patterns of genes involved in sugar and hormone signaling pathway was plotted as a heat map. Orange represented up-regulated in ES group, and blue represented down-regulated in the ES group. Metabolites that were significantly changed are colored in red and green, red indicates higher content and green indicates lower in ES. Grey color represents undetected metabolites, black represents detected metabolites. The solid and dashed arrows between the two metabolites reference the KEGG pathway map. Asterisks represent the three categories of hub genes determined by connectivity between unigenes and metabolites before.

Supplementary Files

This is a list of supplementary files associated with this preprint. Click to download.

- SupplementFigure.docx
- Supplementtable.xlsx